

Adsorption of CO and NO on Ceria- and Pt-Supported TiO₂: *In Situ* FTIR Study

Zeinhom M. El-Bahy^{1,2}

¹Chemistry Department, Faculty of Science, Taif University, Taif, Saudi Arabia

²Chemistry Department, Faculty of Science, Al-Azhar University, Cairo, Egypt

Email: zeinelbahy2020@yahoo.com

Received June 19, 2013; revised August 8, 2013; accepted September 2, 2013

Copyright © 2013 Zeinhom M. El-Bahy. This is an open access article distributed under the Creative Commons Attribution License, which permits unrestricted use, distribution, and reproduction in any medium, provided the original work is properly cited.

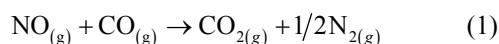
ABSTRACT

Pt/TiO₂, Ce/TiO₂ and binary system PtCe/TiO₂ catalysts were prepared by impregnation method and the structural properties of these catalysts were investigated by means of XRD, CO-TPD and UV-vis diffuse reflectance spectroscopy. As investigated by XRD, the composition of the prepared samples anatase and rutile phases with higher amount of anatase phase and its particle size was in the range of 19 - 22 nm. The band gap also decreased from 3.1 to 2.85 after addition of metal to TiO₂. The adsorption and interaction properties of NO and/or CO gases were monitored using an *in situ* FTIR technique. The intensity and position of the infrared peaks were strongly dependent on the composition of the catalyst. In presence of Pt, the main oxidative reductive products of (NO + CO) are CO₂ and NCO complex. The formation of NCO depends on not only the presence of platinum in the catalyst but also the presence of Lewis acid sites which is Ti⁴⁺ in this study. However, the interaction between NO and CO gases increased in presence of CeO₂. The optimum Ce content in PtCe/TiO₂ was 0.1% (Ce/TiO₂) at which the maximum peak intensity was observed for NCO and CO₂.

Keywords: *In Situ* FTIR; NO Reduction; CO Oxidation; TPD-CO; Platinum-Cerium

1. Introduction

The importance of environmental gas monitoring and controlling is now recognized as an important area to diminish the hazardous chemical vapors present beyond specified levels. CO and NO are known to be extremely harmful to the human body and also a main cause of air pollution since they are two of the most hazardous products released in car exhausts [1]. The best employed methods for eliminating NO and CO are the catalytic reductive and oxidative mechanisms, respectively. Both CO and NO are used as common probe molecules in surface science to obtain fundamental information about the gas-surface interactions, adsorption sites, and reactive dynamics on variety of metals [2]. One of the most important reactions in automobile exhaust catalysis is the reaction between NO and CO over metal oxide surfaces:



Rhodium, platinum and palladium are mostly used to catalyze the reaction in Equation (1) [3]. A Pt/TiO₂ sample has been studied by adsorption and co-adsorption of CO + NO [4]. The activity of Rh supported on the ceria doped titania was investigated and it was found that the

presence of ceria favors the Rh dispersion [5]. González *et al.* [6] reported that Pt supported on Ce-modified TiO₂ support exhibited better activity for water gas shift reaction than those corresponding to individual CeO₂ and TiO₂-supported catalysts. These catalysts were prepared by using metal/Ti ratios of 0.5 for Pt/Ti and 0.005 - 0.07 for Ce/Ti. It will be important to prepare Ce-promoted Pt/TiO₂ catalyst and test it for NO + CO adsorption and interaction as an oxidative/reductive catalytic method for harmful gas removal.

In situ IR spectroscopy study of adsorbed probe molecules, especially of CO, is very useful for the characterization of solid surfaces and gives a unique possibility to characterize the coordination state and electrophilic properties of accessible sites [7]. Activity measurements, when coupled with the physicochemical characterization of catalysts suggest that the modifications in the surface reducibility of the support play an essential role in the enhancement of activity and stability observed when Pt-modified TiO₂ was promoted with CeO₂. Hence, testing the gas interaction over the reduced catalyst should be informative.

The purpose of the present work is to investigate the

effect of cerium oxide addition on the structure and adsorption properties of titania-supported platinum catalyst. CO and/or NO were admitted to the prepared catalysts and the interaction of admitted gases over the catalysts surface was monitored by *in situ* FTIR spectroscopy technique. X-ray diffraction (XRD), Temperature Programmed Desorption (TPD) of CO and Diffuse reflection spectra (UV) were used for solid characterization.

2. Experimental

2.1. Catalyst Preparation

Analytical grade reagents, $\text{Pt}(\text{NH}_3)_4\text{Cl}_2 \cdot \text{H}_2\text{O}$, $\text{Ce}(\text{NO}_3)_3 \cdot 6\text{H}_2\text{O}$ and TiO_2 (Degussa P25, known as a commonly used photocatalyst), were employed as starting materials in this study. The metal supported TiO_2 nanoparticles were prepared by the incipient wetness impregnation method. TiO_2 (4 g) was placed and stirred in water to form a homogenous suspension. A proper amount of an aqueous solution of Pt^{2+} , Ce^{3+} and ($\text{Pt}^{2+} + \text{Ce}^{3+}$) was added to TiO_2 suspension to form the required Pt, Ce, and (Pt + Ce)/ TiO_2 ratios, respectively. The molar ratio Pt/Ti was fixed at 1% and Ce/Ti was changed in the range of 0.05% - 1%. The Pt, Ce and (Pt + Ce) supported TiO_2 precursors slurry were refluxed at 80°C with continuous stirring for 3 h. After impregnation the water was allowed to evaporate using rotary evaporator and the residues were dried at 110°C over night. The obtained solids were then calcined at 500°C in air for 3 h with ramp rate of $2^\circ\text{C}/\text{min}$. The samples were referred to as Pt/ TiO_2 , Ce_x/TiO_2 and $\text{PtCe}_x/\text{TiO}_2$ for Pt, Ce and PtCe-supported titania, where x denotes to the Ce/Ti ratio.

2.2. Catalysts Characterizations

X-ray diffraction (XRD) technique was used to determine the bulk crystalline structures of the prepared catalysts. The XRD patterns were obtained with an x-ray diffractometer, D8 Advance (Bruker axs), with a Cu $K\alpha$ radiation source (30 kV and 20 mA) in the 2θ range of $20^\circ - 60^\circ$. The average crystallite size (D) of the obtained powders was calculated by Hall-equation-Scherrer's formula $D = 0.9\lambda/\beta\cos\theta$ [8]; where λ represents the x-ray wavelength (1.54 Å), θ is the Bragg's angle and β (in radians) is the pure full width of the fraction line at half of the maximum capacity.

Temperature Programmed Desorption (TPD) experiments were carried out using CO gas in a fixed-bed reactor system. Before TPD measurements, the catalyst (30 mg) was treated at 500°C for 1 h in air. Then the heated sample was evacuated for 1 h at the same temperature under vacuum (10^{-4} torr). The sample was then cooled under the same pressure until room temperature and then an amount of CO gas with partial pressure of 7 torr was added and left to equilibrate for 30 min. The sample was

then degassed for 1 h at room temperature. The degassed CO molecules ($m/z = 28$) were monitored by a gas desorption analyzer (ANELVA, M-QA100TS) equipped with a quadruple mass analyzer in a high-vacuum chamber of 7.5×10^{-9} torr range. TPD profiles were recorded by linear heating of the samples from 25°C to 750°C at constant ramp rate of $5^\circ/\text{min}$.

The UV-vis diffuse reflectance spectra of various samples in the 700 - 200 nm range were obtained using a Jasco V-570 (serial number, C29635) spectrophotometer equipped with a diffuse reflectance attachment, using BaSO_4 as a reference.

2.3. Gas Adsorption and Catalytic Activity Measurements

In situ FTIR spectra of CO and/or NO adsorption (7 torr of each) were recorded using JASCO FTIR-660 Plus. Briefly, 15 - 20 mg/cm^2 self-supporting pellets of the catalyst powder were prepared and treated directly in the purpose-made IR quartz cell equipped with CaCl_2 windows. The IR cell was connected to a static vacuum-adsorption system with a residual pressure below 10^{-4} torr. The samples were heated at 500°C for 2 h in air followed by 1 h evacuation at same temperature. Then the catalysts were cooled at room temperature (RT) and at this point, background spectrum was recorded. CO and/or NO gas mixtures were then admitted. The gases were used in equal partial pressure of 7 torr of each (CO:NO; 1:1). After gas admission, the cell was left to equilibrate for 20 min at RT after which the spectrum was recorded again. The former spectrum (before gas admission) was subtracted from the latter one (after gas admission) and will be discussed below. To test the adsorption at higher temperature, the temperature of the IR cell, including the sample wafer and the gas mixture, was raised to the desired temperature. It was kept at such temperature for 20 min after which the IR cell was cooled to RT and then the spectrum was recorded, and kept to test the effect of the addition of trace amount of water vapor, it was added in the gas mixture with a ratio of (CO + NO + H_2O ; 7:7:1).

3. Results and Discussions

3.1. Catalyst Characterization

3.1.1. X-Ray Diffraction

XRD was usually used for identification of the crystal phase and estimation of the ratio of the anatase to rutile as well as crystallite size of each phase. **Figure 1** shows the XRD patterns of titania and metal supported TiO_2 catalysts. The patterns proved the presence of both anatase and rutile phases in all samples. The peaks at $2\theta = 26.1$ (101), 38.6 (112), 48.8 (200) and 55° (211) in the spectrum of all samples are easily identified as the crystal

of anatase form [PDF# 84 - 1286], whereas the XRD peaks at $2\theta = 28.2$ (110), 36.9 (101), 42 (111) and 55.9° (211) are easily taken as the crystal of rutile form [PDF# 88 - 1175]. In addition, small peak at $2\theta = 37.9^\circ$ due to titanate ($\text{H}_2\text{Ti}_4\text{O}_9 \cdot 1.9\text{H}_2\text{O}$) [PDF# 39 - 0040] was observed and increased in samples containing Pt. The patterns did not show any peaks for loaded metal oxides, indicating that these metal oxides were well dispersed in all cases. The XRD intensities of the anatase peak at $2\theta = 26.1^\circ$ and the rutile peak $2\theta = 28.2^\circ$ were also analyzed to determine the percentage of anatase in the samples from the respective integrated XRD peak intensities using the following equation [9]: $X (\%) = 100/(1 + 1.265I_R/I_A)$, where X is the weight percentage of anatase in the sample; I_A represents the intensity of the anatase peak at $2\theta = 26.12^\circ$ and I_R is that of the rutile peak at $2\theta = 28.2^\circ$. The patterns in **Figure 1** and the data listed in **Table 1** show that most of the structure of the prepared samples is anatase form. It could be seen that the presence of other metal oxides such as Pt or Ce oxides increased the anatase ratio. These data demonstrated that the employed metals could inhibit the transformation from anatase to rutile. These observations are in good agreement with previous reports [10]. The particle size of the prepared

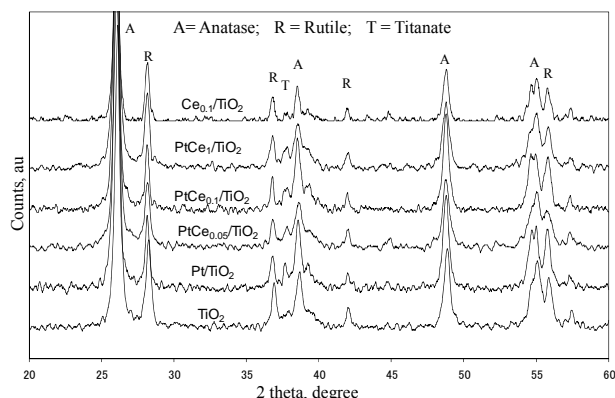


Figure 1. X-ray powder diffraction patterns of parent TiO_2 and Pt and Ce-supported TiO_2 catalysts.

Table 1. Crystallite size of parent TiO_2 and Ce- and Pt-supported TiO_2 catalysts.

Catalyst	Phase % by XRD		Crystallite size, nm		Band gap, eV
	Anatase	Rutime	Anatase,	Rutile	
TiO_2	72.6	27.4	19.9	25.1	3.1
PtTiO_2	80.0	20.0	21.5	27.2	2.95
$\text{Ce}_{0.1}\text{TiO}_2$	72.3	27.7	20.6	25.7	2.85
$\text{PtCe}_{0.05}\text{TiO}_2$	76.0	24.0	17.8	24.9	-
$\text{PtCe}_{0.1}\text{TiO}_2$	82.3	17.7	22.6	34.9	2.9
$\text{PtCe}_1\text{TiO}_2$	74.6	25.4	19.4	26.7	

solids was calculated using Scherrer's equation. **Table 1** shows the average crystallite size for both anatase ($2\theta = 25.9^\circ$, 38.5° and 48.7°) and rutile ($2\theta = 28.1^\circ$, 36.7° and 55.9°) phases. The particle size was found to be in the range of 19 - 22 nm for anatase phase while it was 25 - 35 nm for rutile phase.

3.1.2. Temperature Programmed Desorption (TPD)

The TPD spectra after CO adsorption of pure TiO_2 and the prepared catalysts are shown in **Figure 2**. The magnitude of the desorption maxima differs somewhat between the metal-free and supported TiO_2 samples. The CO peak maximum for pure TiO_2 is observed at approximately $\approx 540^\circ\text{C}$. This profile changed after loading of Pt and Ce to TiO_2 surface. In case of Pt/TiO_2 , three CO desorption peaks can be distinguished at $\approx 175^\circ\text{C}$, 560°C and $\approx 695^\circ\text{C}$. However, $\text{Ce}_{0.1}\text{TiO}_2$ showed one CO desorption peak at $\approx 615^\circ\text{C}$. This indicates that CeO_2 does not show any CO adsorption which in accordance with other reports [11], though it caused the shift of CO desorption peak to higher temperature compared to that of Ce-free TiO_2 . Bimetallic $\text{PtCe}_{0.1}\text{TiO}_2$ sample showed two desorption peaks at $\approx 125^\circ\text{C}$ and another one at $\approx 560^\circ\text{C}$. The CO desorption temperatures of $\text{Ce}_{0.1}\text{TiO}_2$ and Pt/TiO_2 are anomalously high comparing to the desorption values of TiO_2 *i.e.* these samples have higher molecular CO desorption energy due to the creation of strong basic sites. The strong basic sites of Pt/TiO_2 attenuated in presence of Ce in $\text{Pt/Ce}_{0.1}\text{TiO}_2$. Such attenuation may be due to site-blocking effect of the other metal ion (Ce) which occupies adsorption sites for CO and suppresses CO chemisorptions [12]. The data showed that the apparent area under peaks for Pt/TiO_2 is larger than that for $\text{PtCe}_{0.1}\text{TiO}_2$ indicating that the dispersion of Pt in the former is higher than that in the later [11].

3.1.3. UV-vis Diffuse Reflectance

Diffuse reflection spectra of pure TiO_2 and metal sup-

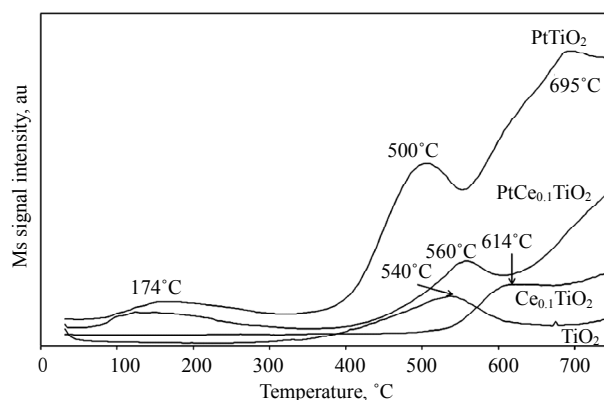


Figure 2. CO-TPD profiles of parent TiO_2 and the prepared solids.

ported catalysts are shown in **Figure 3**. Generally, anatase-type TiO_2 crystalline has a strong absorption edge below 380 nm [13]. From the presented profiles, the prepared samples showed mainly anatase structure which is consistent with XRD patterns. In addition, after mounting metal ions to the surface of TiO_2 , the slopes of the absorption edges slightly changed compared with pure TiO_2 . The band gap energy was estimated with the Kubelka-Munk method using diffuse reflectance spectra [14]. After calculations, unpromoted titania has a typical band gap of 3.1 eV, whereas the band gap magnitude of the metal supported titania decreased slightly; that is 2.95, 2.9 and 2.85 eV for Pt/TiO_2 , $\text{PtCe}_{0.1}/\text{TiO}_2$ and $\text{Ce}_{0.1}/\text{TiO}_2$, respectively, as listed in **Table 1**. These results disclose one crucial fact that the employed metals interact with TiO_2 and hence the band gap changed.

3.2. Adsorption of CO on the Prepared Samples

The results of CO adsorption (7 torr) over the pure TiO_2 and metal loaded TiO_2 at RT in the range of 2400 - 1100 cm^{-1} are presented in **Figure 4**. Since the absorptions regions of Pt^{n+} -CO and Ti^{4+} -CO carbonyls may overlap, it was important to study the adsorption of CO over metal free TiO_2 . Adsorption of CO on TiO_2 sample, **Figure 4(a)**, leads to the appearance of two bands, at 2205 and 2187 cm^{-1} which are produced by carbonyl complexes of two types of coordinatively unsaturated sites (c.u.s.) Ti^{4+} cations (α - and β - Ti^{4+} , respectively) [15]. The β - Ti^{4+} sites are the highly unsaturated sites due to kinks and corners [5]. It was reported that the IR bands in the 1600 - 1200 cm^{-1} is mainly due to the formation of large number of different adsorbed carbonate species. In addition, formate (HCOO^-) species can be excluded because they are formed at relatively high temperatures (227°C) [16]. Consequently, the existence of different bands in the region of 1600 - 1220 cm^{-1} (1356, 1435 and 1533 cm^{-1}) under the present adsorption conditions may

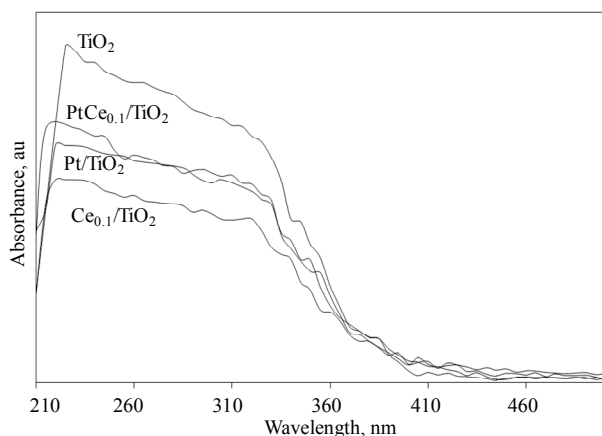


Figure 3. UV-vis diffuse reflectance of parent TiO_2 and the prepared catalysts.

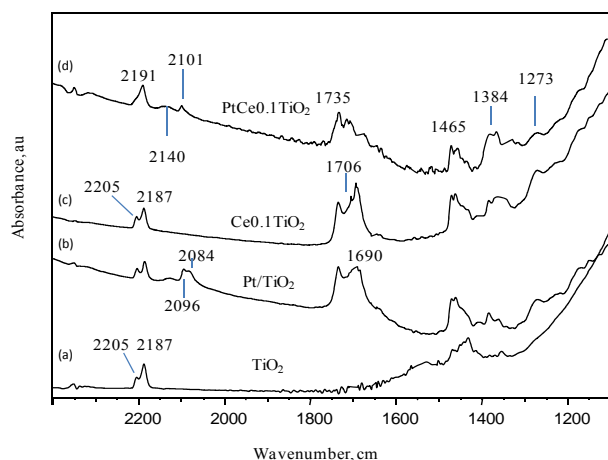


Figure 4. FTIR spectra after admission of CO (7 torr) over parent TiO_2 and Pt and Ce-supported TiO_2 .

be taken with a higher degree of confidence to $\nu_{\text{as}}(\text{COO}^-)$ and $\nu_{\text{s}}(\text{COO}^-)$ with a geometry change of these species [16]. This indicates that CO can be converted to carbonate species over TiO_2 even at RT. Indeed, the formation of carbonate has been previously confirmed spectroscopically on surfaces of various oxides as a result of the adsorption of CO on coordinatively unsaturated Lewis acid-base pair sites ($\text{M}^{n+}\text{-O}^{2-}$), similar to the results reported for CO adsorption over ZrO_2 [17], PrO_2 [16] or PtY [18].

To reveal the effect of Ce and Pt loading on TiO_2 surface, the in-situ FTIR of CO adsorption on the samples $\text{Ce}_{0.1}/\text{TiO}_2$, Pt/TiO_2 and $\text{PtCe}_{0.1}/\text{TiO}_2$ was performed and the results are presented in **Figures 4(b)-(d)** as well. In case of Pt/TiO_2 , the peaks characteristic of Ti^{4+} at 2189 and 2205 cm^{-1} were observed besides three peaks at 2082, 2096 and 2128 cm^{-1} which are attributed to linearly adsorbed $\text{Pt}^0\text{-CO}$, $\text{Pt}^+\text{-CO}$ and $\text{Pt}^{2+}\text{-CO}$, respectively [18,19]. The adsorption peaks at 1276, 1362 and 1467, 1690 cm^{-1} are also related to the presence of carbonate species which are formed on $\text{Pt}^{n+}\text{-O}^{2-}$ or $\text{Ti}^{4+}\text{-O}^{2-}$ sites. A peak at 1737 cm^{-1} was observed which is due to carboxylate (COO^-) species [20].

For $\text{Ce}_{0.1}/\text{TiO}_2$ catalyst, there were only two peaks at 2187 and 2205 cm^{-1} . It was reported in literature that, two weak peaks at 2177 and 2156 cm^{-1} were found for CO adsorbed on ceria after evacuation at liquid nitrogen temperature [21]. However, our adsorption temperature is much higher than -196°C , so it is expected to not observe any of CO adsorption peaks on ceria. Consequently, the peaks at 2187 and 2205 cm^{-1} are characteristic of CO adsorption on β - and α - Ti^{4+} sites, respectively. This is also in agreement with the work of Chen *et al.* [22]. This spectrum also shows peaks characteristic of CO oxidation products such as ($-\text{COO}^-$) at 1735 cm^{-1} and carbonate species at 1700, 1694, 1467, 1384 and 1273 cm^{-1} .

Finally, with respect to $\text{PtCe}_{0.1}/\text{TiO}_2$ spectrum, only one peak due to CO adsorption on $\beta\text{-Ti}^{4+}$ was observed at 2192 cm^{-1} , however, the CO adsorption peak at 2205 cm^{-1} characteristic of $\alpha\text{-Ti}^{4+}$ was not observed. Additionally, the sample presented small peaks at 2101 and 2140 cm^{-1} which are due to $\text{Pt}^+\text{-CO}$ and $\text{Pt}^{2+}\text{-CO}$, respectively. It is noticed that, these peaks are located at higher frequencies than those in Pt/TiO_2 . This shift may be due to the presence of Ce^{4+} which decreases the electron density on Pt^{n+} species. It is noteworthy to mention that, bridged $\text{Pt}_2(\text{CO})$ species were not observed in all the samples in CO adsorption experiments. This phenomenon means that Pt particles are mostly isolated with high dispersion over the surface and this is in good accordance with XRD data. The spectrum of CO adsorption on $\text{PtCe}_{0.1}/\text{TiO}_2$ showed mostly the same carbonate like species in the frequency range of $1800 - 1100\text{ cm}^{-1}$.

3.3. Adsorption of NO + CO on the Prepared Samples

The spectra (not shown) collected after exposure of the prepared catalysts to NO gas (7 torr) did not lead to the formation of any nitrosyls complexes adsorbed on the metal loaded TiO_2 . This was not consistent with the previous literature [23] and it may be due to the low concentration of admitted NO gas and the relatively high adsorption temperatures.

3.3.1. In Situ FTIR Results of NO and CO Co-Adsorption on TiO_2 Catalyst

Figure 5 shows the spectra of TiO_2 ($2400 - 1100\text{ cm}^{-1}$) after admission of gas mixture of CO + NO (7:7) at different temperatures in the range of RT to 200°C . At RT, it was observed in the spectrum that, two peaks at 2187 and 2350 cm^{-1} were detected after 20 min of gas expo-

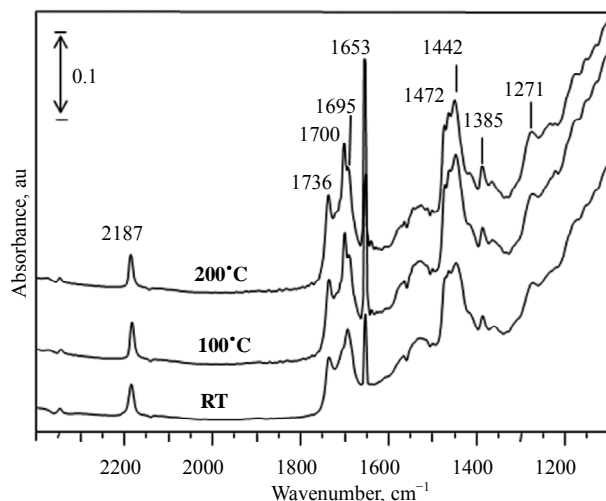


Figure 5. FTIR spectra after admission of gas mixture (NO + CO; 7:7) on TiO_2 at different temperatures.

sure. Based on previous literature reports, the former band is assigned to CO adsorbed on $\beta\text{-Ti}^{4+}$ cations and the latter one is attributed to CO_2 [4-6]. These results indicate that some fraction of the adsorbed CO molecules undergo oxidation to CO_2 upon the contact with gas phase NO through TiO_2 surface even at room temperature.

Additionally, a peak characteristic of carboxylate species (COO^-) was noticed at 1736 cm^{-1} [20]. Carbonate species were detected at several positions such as 1700 cm^{-1} , however, the corresponding asymmetric $\nu_{\text{as}}(\text{COO}^-)$ peaks for these species are detected at 1470 and 1442 cm^{-1} . Different types of carbonates species exhibited peaks at 1700 , 1531 , 1385 and 1271 cm^{-1} [24]. The peak at 1695 and 1470 cm^{-1} may be due to carbonate species [24] or ν_{s} and ν_{as} of NH_4^+ [25,26]. However, we could not notice any vibrations in the range of $2600 - 3000\text{ cm}^{-1}$ due to adsorbed NH_3 . Therefore, the absorption peaks at 1695 and 1470 cm^{-1} are due to carbonate species. When the temperature of the infrared cell containing wafer was increased to 100 and 200°C while keeping the same gas mixture CO + NO, the same group of bands was noticed with an increase in the intensity of the peaks characteristic of CO oxidation products. This indicates the increase of the possibility of CO oxidation and NO reduction with increasing the wafer temperature. It is noticed that, after admission of NO gas together with CO, the peak at 2205 cm^{-1} which is due to $\alpha\text{-Ti}^{4+}\text{-CO}$ was not observed. This may be due to the increase in the coverage of strongly adsorbed carbonate species resulting from CO oxidation. The peak at 1653 cm^{-1} is due to $\delta(\text{HOH})$ mode of adsorbed molecular water [27].

3.3.2. In Situ FTIR Results of NO and CO Co-Adsorption with Pt/TiO_2 Catalyst

After recording the spectrum of the sample prior admission of gas mixture, the IR spectra of CO + NO (7:7) adsorption over platinum supported TiO_2 in the range of $2400 - 1100\text{ cm}^{-1}$ at different temperatures (RT - 200°C) are shown in Figure 6. After 20 min of admission of gas mixture at RT, the spectrum presented peaks due to $\alpha\text{-Ti}^{4+}\text{-CO}$ at 2205 cm^{-1} , $\beta\text{-Ti}^{4+}\text{-CO}$ at 2187 cm^{-1} and the peak at 2077 cm^{-1} assigned to singleton frequency of CO molecules linearly adsorbed on-top metallic Pt atoms ($\text{Pt}^0\text{-CO}$) [28]. These results indicate that some fraction of the Pt^{2+} species, which are initially present in the sample, underwent reduction to metallic Pt at RT in presence of CO gas.

Other peaks characteristic of the CO oxidation products such as physisorbed CO_2 at 2350 cm^{-1} and a group of peaks characteristic of (-COO^-) species at 1737 cm^{-1} and the peaks at 1693 , 1582 , 1461 , 1386 and 1276 cm^{-1} were recorded and attributed to carbonate species adsorbed on different sites or in different geometry [16].

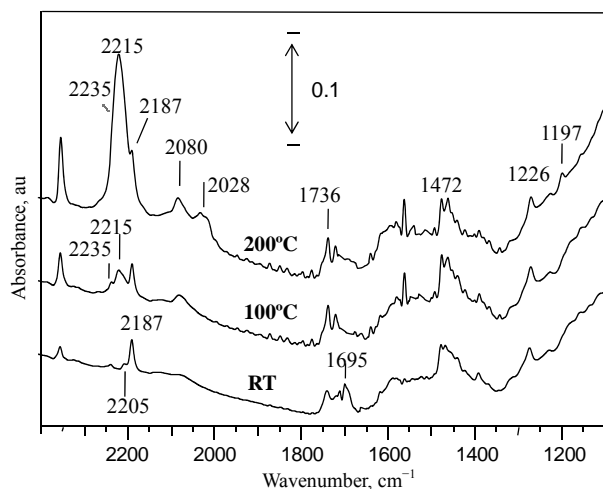
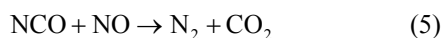
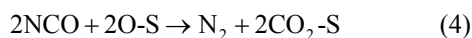
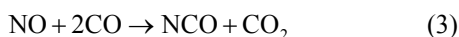


Figure 6. FTIR spectra after admission of gas mixture (NO + CO; 7:7) on Pt/TiO₂ at different temperatures.

The intensity of these peaks increases with increasing temperature from RT to 200°C.

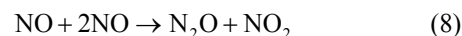
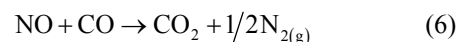
In addition to the oxidation products of CO, the appearance of a new small peak at 2236 cm⁻¹ was noticed in the collected spectra (at RT) in this case, **Figure 6**. It should be mentioned that, the peak at 2236 cm⁻¹ was not observed when only one reactant, either CO or NO, was admitted to the catalyst surface. It was only observed when CO + NO were present simultaneously. Also, it was not observed when CO + NO were admitted to Pt-free catalysts. Based on previous literature reports [29], this band can be assigned to the asymmetric vibration of a surface NCO species as presented in Equation (3). Although, the mechanism of NCO formation is not clear until now, the assumption in Equation (3) is supported by the presence of physisorbed CO₂ [3]:



According to previously published data, the formation of isocyanate requires the presence of platinum group metals in the catalyst [30-32]. In addition, the process of NCO formation is typically followed by the migration of these species from the metal sites to the support which means that NCO may be adsorbed on Ti⁴⁺ sites. The formation of NCO may lead to the formation of CO₂ via the reaction with the oxygen of oxide species (Equation (4)) or with the reaction with NO molecules (Equation (5)) [29].

Elevating the temperature of the FTIR cell to 100°C and 200°C leads to the increase of CO₂ peak at 2350 cm⁻¹, **Figure 6**. An increase of the intensity of the peak at 2080 cm⁻¹ was detected besides a development of a new peak at 2028 cm⁻¹. These two peaks can be most probably

assigned to symmetric and asymmetric stretching, respectively, of gym-dicarbonyl species (CO-Pt⁰-CO). At 200°C, the peak at 2236 cm⁻¹ became very intense and centered at 2215 cm⁻¹. Besides the possibility of the presence of absorption peak characteristic of α-Ti⁴⁺-CO (2205 cm⁻¹), the shape of this peak suggests that at least three overlapping components are present which indicates that several types of adsorbed species on Pt/TiO₂ catalyst surface are located in this wide peak. The first component can be distinguished at 2187 cm⁻¹ which was attributed to CO adsorption on β-Ti⁴⁺. The second component is centered at 2215 cm⁻¹ which is attributed to isocyanate species (NCO) [30]. The last component is located at ≈2235 cm⁻¹ and can be assigned NCO adsorbed on different sites or to nitrous oxide (N₂O) [33]. N₂O may be formed either by reduction of NO by CO Equations (6) and (7) or by disproportionation process as Equation (8). It was reported that, N₂O is easily formed on Ti³⁺ and Ce³⁺ sites formed after reduction of the catalyst by H₂ gas [5]. In this work, this band was not observed after admitting NO + CO to the reduced catalyst as will be shown later on. This indicates that the peak at 2235 cm⁻¹ is most probably assigned to NCO. Close inspection of **Figure 6**, it can be inferred that, the peak assigned to physisorbed CO₂ gas (2350 cm⁻¹) increases in parallel with NCO (2216 cm⁻¹) species. This may point to the formation of NCO through reduction (Equations (3)-(5)) rather than disproportionation (Equation (8)). The presence of other NO-derived species at Pt/TiO₂ can be inferred from the small peaks at 1226 and 1197 cm⁻¹. For example, the peak at 1200 cm⁻¹ could be associated with a chelating nitrite species (NO_x) [15].



It is well known that, isocyanate, nitrous oxide or nitrogen dioxide are proposed to be connected to the reaction mechanism of NO-CO reaction [34]. This result was also noticed by Keiski *et al.* [3] since they detected an increase of isocyanate complex peak after heating at 300°C. They reported that, the formation of NCO surface complexes over CeO₂ catalyst required that the surface of the catalyst was first occupied by NO. In our case, the formation of NCO species did not require NO admission prior to CO. However it was formed just after NO + CO gases are admitted together at relatively low temperature (RT).

3.3.3. *In Situ* FTIR Results of NO and CO

Co-Adsorption with Ce_{0.1}/TiO₂ Catalyst

In situ FT-IR spectra (2400 - 1100 cm⁻¹) of the co-adsorption of NO and CO over Ce_{0.1}/TiO₂ catalyst at RT

was shown in **Figure 7**. After exposure of NO + CO mixtures to the catalyst surface and equilibrate for 20 min, the peaks at 2189 cm^{-1} which are due to CO adsorption over $\beta\text{-Ti}^{4+}$ was observed. Other peaks characteristic of CO oxidation products were detected at 1740, 1700, 1465, 1362 and 1276 cm^{-1} . The peak at 1740 cm^{-1} is attributed to carboxylate (COO^-) species. The other peaks are due to carbonate species adsorbed at different sites or adsorbed in different geometry [16]. With the stepwise increasing temperature from RT to 200°C , the intensity of these peaks slightly increases with a parallel slight increase of the peak at 2350 cm^{-1} which is due to physically adsorbed CO_2 . Since NCO was not observed at all, it can be concluded that CO_2 was formed due to the oxidation of CO with lattice oxygen. Moreover, NO oxidation product was detected at 1622 cm^{-1} due to bridged nitrate species [27]. A peak at 1653 cm^{-1} was detected and assigned to $\delta(\text{HOH})$.

By careful examination of the spectra in **Figure 7**, it can be noticed that, there were some differences between the spectra obtained after admission of NO + CO gas mixture to Pt-containing and Ce-containing catalysts as follows:

- The $\alpha\text{-Ti}^{4+}$ -CO adsorption peak disappeared.
- The Pt^{n+} -CO adsorption peaks disappeared.
- An oxidation product of NO was observed at 1617 cm^{-1} which is assigned to NO_2 [3] and a peak at 1360 cm^{-1} due to nitrate species [15,35].
- Due to the absence of platinum group metals, the spectra did not show any peaks characteristic of NCO species [29].

3.3.4. In Situ FTIR Results of NO + CO Co-Adsorption with $\text{PtCe}_{0.1}/\text{TiO}_2$ Catalyst

Figure 8 reports the evolution of the adsorbed gaseous

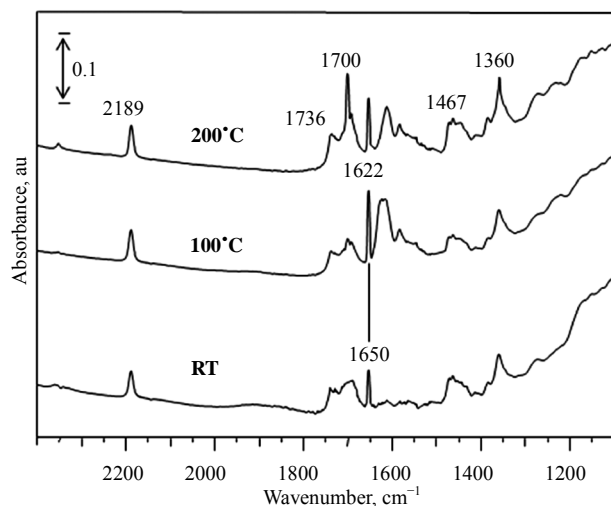


Figure 7. FTIR spectra after admission of gas mixture (NO + CO; 7:7) on $\text{Ce}_{0.1}/\text{TiO}_2$ at different temperatures.

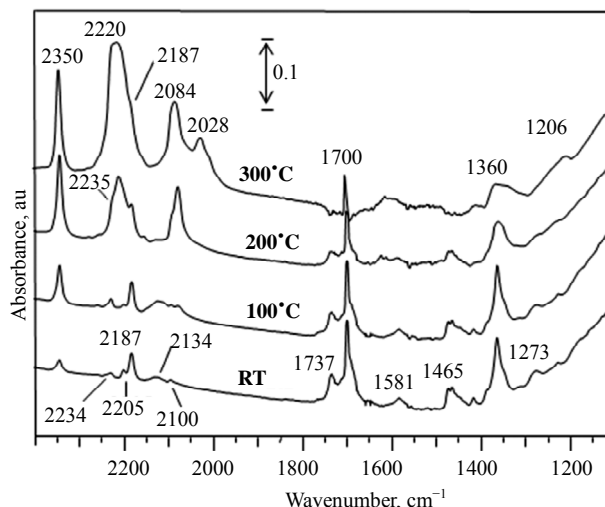


Figure 8. FTIR spectra after admission of gas mixture (NO + CO; 7:7) on $\text{PtCe}_{0.1}/\text{TiO}_2$ at different temperatures.

species under the reaction conditions from RT to 300°C over the bimetallic Ce- and Pt-supported on TiO_2 ($\text{PtCe}_{0.1}/\text{TiO}_2$) catalyst. At RT, the spectrum shows peaks at 2189 and 2205 cm^{-1} which are characteristic of CO adsorbed over Ti^{4+} sites as previously mentioned. Other bands at 2134 and 2100 cm^{-1} are due to carbonyl complexes formed with the participation of platinum cations Pt^{2+} -CO and Pt^+ -CO, respectively [36-38]. The spectrum shows also a small peak at 2234 cm^{-1} due to NCO species.

The spectrum showed also peaks due to CO and NO interaction over the $\text{PtCe}_{0.1}/\text{TiO}_2$ catalyst surface. CO Oxidation products were observed as strong peak at 2350 cm^{-1} due to physically adsorbed CO_2 . Other peaks at 1737 cm^{-1} due to (COO^-) species and 1700, 1465 and 1273 cm^{-1} due to carbonate species adsorbed on different sites were observed. Some NO oxidation derivatives were detected as well at 1581 cm^{-1} due to bidentate NO_3^- and at 1206 cm^{-1} due to NO_x^- [15].

It is clear that there are drastic changes in the spectra with elevation of the temperature of sample wafer and IR cell including adsorbed CO on Pt^{n+} sites and CO + NO oxidation reduction derivatives. These changes can be summarized as:

- The peaks characteristic of Pt^0 -CO increased indicating further reduction of Pt^{n+} sited with CO at high temperature.
- A new peak at 2028 cm^{-1} appeared. This peak was detected (small intensity) in case of Pt/TiO_2 catalyst. Hence it can be assigned to CO adsorbed on Pt^0 sites. This also ensures the possibility of Pt^{n+} reduction in presence of CO at high temperature.
- Increase of CO_2 peak on the expense of other CO oxidation products which means that CO_2 is the predominant CO oxidation product at high temperature.

Moreover, this data points to the fact that, carbonate species are the intermediates in CO oxidation to CO₂.

- The peak centered at 2220 cm⁻¹ may be composed of three components at 2187 cm⁻¹ (due to β-Ti⁴⁺-CO), a peak at 2220 and 2235 cm⁻¹ (due to NCO species). CO absorption peak at α-Ti⁴⁺ may be one of these components too.
- Increase of the peak characteristic of NCO with a simultaneous decrease of each of the peaks at 1360 cm⁻¹ (NO₃⁻), 1737 cm⁻¹ (COO⁻) and 1700, 1465 and 1273 cm⁻¹ may point to the reaction of these species to form NCO and CO₂. However the exact mechanism of these reactions is not exactly known. It was reported in literature that, the addition of cerium to Rh/TiO₂ [5] and Rh/Al₂O₃ [39,40] enhances the NO dissociation rate at quite low temperatures and suppresses the N₂O formation. Consequently, isocyanate is the dominant product that arises after the co-adsorption of NO + CO gas to the PtCe/TiO₂.

Examining the results of NO + CO adsorption over Pt/TiO₂ and Ce_{0.1}/TiO₂, **Figure 8**, points to the fact that, NCO can be formed only on the surface of Pt/TiO₂ but not on Ce_{0.1}/TiO₂ surface. This is in good agreement with the previously reported data [3]. In general, it is believed that NCO formation occurs on Lewis acid sites via the reaction of CO and nitrogen atoms that is formed by NO dissociation. It has also been suggested that the process of NCO formation is typically followed by the migration of these species from the metal sites to the support where such species are more stable [28]. Additionally, investigating **Figures 6** and **8**, it is observed that, the intensity of the peaks characteristic of CO₂, NCO are higher in **Figure 8** (PtCe_{0.1}/TiO₂). It can be concluded that, Ce enhanced the formation of NCO and CO₂. This may be due to the availability of more Lewis acid sites which is necessary to form NCO [28]. It will be interesting to eliminate the Lewis acid sites by reducing one of the employed catalysts and check the possibility of the formation of isocyanate species.

3.3.5. In Situ FTIR Results of NO + CO Co-Adsorption with Reduced PtCe_{0.1}/TiO₂ Catalyst

It is well known that, the capability of the oxidized and the reduced forms of platinum are different towards the CO or NO adsorption and interaction on its surface. Therefore, PtCe_{0.1}/TiO₂ was reduced by H₂ gas at 400°C for 30 min in static vacuum system in presence of liquid nitrogen trap. The reduced catalyst PtCe_{0.1}/TiO₂ was exposed to NO + CO gas mixture at RT and left for 20 min before spectrum measurements. The changes in the spectra (2400 - 1100 cm⁻¹) as a function of wafer temperature were recorded and shown in **Figure 9**. Notably, no peak absorptions belonging to Ti⁴⁺-CO were noticed even after

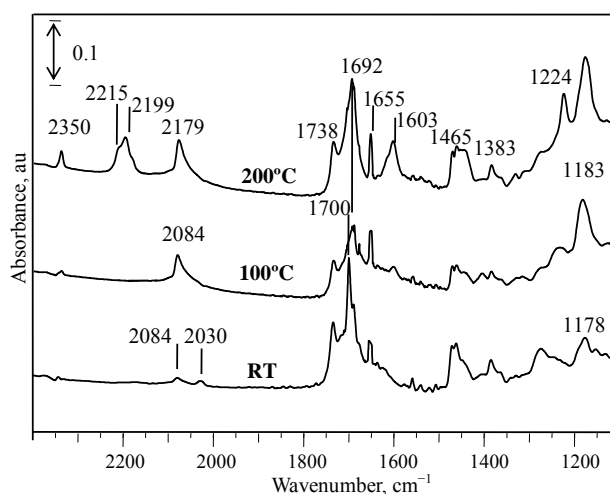


Figure 9. FTIR spectra after admission of gas mixture (NO + CO; 7:7) on reduced PtCe_{0.1}/TiO₂ at different temperatures.

raising the IR cell temperature to 100°C, however, two components were observed at 2199 and 2215 cm⁻¹ due to CO adsorption on Ti⁴⁺ sites and NCO, respectively, at 200°C. Similar to NO + CO adsorption over reduced Rh/Al₂O₃ [3], gym-dicarbonyl species were observed at 2084 and 2030 cm⁻¹ after admission of gases at RT. These peaks are characteristic of symmetric and asymmetric stretching of C-O bond, respectively, of adsorbed CO on Pt sites. The absorption peak related to asymmetric C-O bond (2030 cm⁻¹) disappears, while the intensity of symmetric C-O bond (2084 cm⁻¹) increased with blue shift to lower wavelength (2079 cm⁻¹) indicating the decrease of CO concentration. Increasing the wafer temperature to 200°C leads to an increase of the absorption peak at 2345 cm⁻¹ which is characteristic of physisorbed CO₂. The appearance of CO₂ was accompanied by a decrease of gym-dicarbonyl species which points out to the transformation of CO to CO₂.

In the low wavelength region (1800 - 1100 cm⁻¹), different peaks were attributed to CO oxidation species were observed at 1738 cm⁻¹ due to carboxylate species (COO⁻) and the peaks at 1700, 1582, 1472, 1383 and 1276 cm⁻¹ were recorded and attributed to carbonate species adsorbed on different sites. Additionally, the peak at 1655 cm⁻¹ may be due to H₂O vibration or HCO₃⁻. The progress of both 1655 and 1224 cm⁻¹ confirms the assumption that these peaks are related to the presence of asymmetric bicarbonate species (HCO₃⁻) [41] and their intensity increase by increasing the wafer temperature.

Besides the CO oxidation products, NO reduction derivatives were also observed. The small broad peak centered at 2657 cm⁻¹ (not shown) is attributed to physisorbed ammonia (NH₃). This peak did not change even with increasing the IR cell temperature. The peaks at

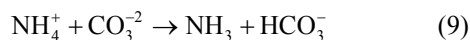
1696 and 1472 cm^{-1} were also observed and they are assigned to the ν_s and ν_{as} vibrations, respectively, of NH_4^+ ions [25,26]. A new peak at 1178 cm^{-1} was noticed after admission of the gas mixture at RT to the reduced catalyst surface. According to Liu *et al.* [35], the peak at 1178 cm^{-1} is due to anionic nitrosyle (NO^-) species. With increasing temperature to 100°C and 200°C, the intensity of this peak increased with a red shift to higher wavelength (1183 cm^{-1}). It is noteworthy to mention that, NH_3 and NO^- were detected only after admission of the gas mixture (NO + CO) over reduced $\text{PtCe}_{0.1}/\text{TiO}_2$ catalyst but not over Pt/TiO_2 , $\text{Ce}_{0.1}/\text{TiO}_2$ or as prepared $\text{PtCe}_{0.1}/\text{TiO}_2$. These data confirms that, at RT, the formation of NCO (as reductive derivative) is preferable over as-prepared Pt-containing catalysts while NH_3 or NO^- is preferable over reduced catalysts.

It is clear that, all the absorption peaks characteristic of C containing species are shifted to lower wavelength with raising temperature. However, the peak at 1692 cm^{-1} , which was detected at 100°C and 200°C, can be assigned to (CO_3^{2-}) rather than (NH_4^+) species.

It is noteworthy to mention that, the absorption peak related to $\text{Pt}^0\text{-CO}$ increased with increasing temperature to 100 and 200°C. Also, two peaks at 2345 and ≈ 2200 cm^{-1} were observed at 200°C. These peaks are attributed to physisorbed CO_2 and NCO species, respectively. The increase of the absorption peak characteristic of $\text{Pt}^0\text{-CO}$ and the increase of the peak characteristic of CO_2 may indicate that carbonate species formed at RT may be reduced once again to CO and forms $\text{Pt}^0\text{-CO}$ or they may be oxidized further to CO_2 which is detected at 200°C. These results confirm the assumption that CO_3^{2-} anion is an intermediate in the oxidation of CO to CO_2 . Furthermore, reduction of NO with CO ($\text{NO}^* + \text{CO}^* \rightarrow \text{NCO}^* + \text{O}^*$) on the reduced catalysts surface occurs only at relatively high temperature (200°C) on the reduced surface. Though, this reaction takes place at RT in the Pt-containing as-prepared catalysts.

It was mentioned earlier that the presence of Pt sites are essential to the formation of NCO. The absence of both the absorption peaks characteristic of $\text{Ti}^{4+}\text{-CO}$ and NCO in the temperature range of RT - 100°C provides clear evidence that Lewis acid sites (most probably Ti^{4+}) is essential for the stabilization of isocyanate species. Nevertheless, NCO species formed at Pt sites can spill onto the support surface where they are accumulated and stabilized [29,30].

The rational increase of the peak characteristic of HCO_3^- with the decrease of NH_4^+ may indicate that bicarbonate species are formed by the interaction between NH_4^+ species and CO_3^{2-} .



3.3.6. *In Situ* FTIR Results of NO + CO Co-Adsorption with $\text{PtCe}_{0.1}/\text{TiO}_2$ Catalyst in Presence of Water Vapor

Addition of trace amount of water vapor increased the activity towards the CO oxidation in presence of Pt and decreased the oxidation temperature as well [18,42-44]. Moreover, the gas exhaust usually contains water vapor and then it will be valuable to add trace amount of H_2O vapor to the gas mixture to detect its effect on the NO + CO interaction. **Figure 10** shows the spectra taken after 20 min of admission of the gas mixture (NO + CO + H_2O ; 7:7:1) over $\text{PtCe}_{0.1}/\text{TiO}_2$ to shade light on the effect of introducing water vapor during NO reduction by CO (more realistic conditions). After adsorption of the gas mixture at RT, several peaks were observed due to CO adsorption over $\text{Pt}^+\text{-CO}$ and $\text{Pt}^0\text{-CO}$ at 2094 and 2072 cm^{-1} , respectively. A new peak at 1840 cm^{-1} due to bridged $\text{Pt}^0\text{-CO-Pt}^0$ was observed [4]. This indicates that the presence of water vapor leads to the decrease of Pt particles dispersion.

With increasing temperature, the intensity of the peak at 2092 cm^{-1} decreases and the peak at 2072 cm^{-1} slightly shifted to lower frequency and even gained some intensity. This phenomenon is, however, most probably due to some reduction of cationic platinum to metal during the CO desorption. Also, at 200°C, small intensity peaks were observed at ≈ 2350 cm^{-1} indicating the formation of physically adsorbed CO_2 . Inspecting of **Figure 10**, isocyanate species NCO (2240 - 2200 cm^{-1}) could not be observed in presence of water which means that the interaction of gas mixture (NO + CO) do not proceed in the pathway to form NCO even at high temperature. The small intensity peaks characteristic of CO_2 may be formed by direct CO oxidation with lattice oxygen. It is clear that the Ti^{4+} sites were not observed except very

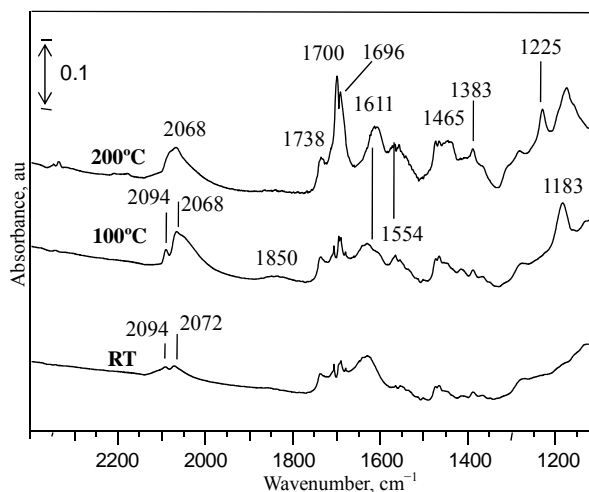


Figure 10. FTIR spectra after admission of gas mixture (NO + CO + H_2O ; 7:7:1) on $\text{PtCe}_{0.1}/\text{TiO}_2$ at different temperatures.

weak peak at 2180 cm^{-1} after raising IR cell temperature to 200°C . This may be due to the competitive adsorption of H_2O and CO over Ti^{4+} sites. The unavailability of Ti^{4+} and the absence of isocyanate species confirm the assumption that, Ti^{4+} sites (Lewis acid) are necessary as hosts for NCO species after their formation over Pt sites.

The spectra were also studied in the frequency range of $1800 - 1100\text{ cm}^{-1}$. Different peaks characteristic of CO oxidation products were observed at 1738 cm^{-1} for carboxylate (COO^-), 1554 and 1225 cm^{-1} for bicarbonate (HCO_3^-) and (1700 , 1611 and 1383 cm^{-1}) for CO_3^{2-} species were detected. Finally, some NO reduction products were also observed at 1696 and 1465 cm^{-1} for NH_4^+ and 1183 cm^{-1} for NO^- . It can be seen that, by increasing the wafer temperature, the peak characteristic of NO^- is red shifted to low wavenumber and the intensity of the peaks characteristic to $\text{CO} + \text{NO}$ oxidative reductive products increased.

3.3.7. Effect of Ce Ratio on the *in Situ* FTIR Results of $\text{NO} + \text{CO}$ Co-Adsorption with $\text{PtCe}_x/\text{TiO}_2$ Catalysts

The influence of the amount of Ce in $\text{PtCe}_x/\text{TiO}_2$ on the $\text{NO} + \text{CO}$ adsorption and interaction on the catalyst surface was studied using the same above-mentioned experimental conditions, except that the ratio of Ce/TiO_2 was changed in the range of 0.05% - 1% . For the sake of simplicity, **Figure 11** shows the spectra recorded after admission of the gas mixture and heating the wafer at 200°C in the range of $2400 - 2000\text{ cm}^{-1}$ since the spectra did not show significant difference below 2000 cm^{-1} (now shown) in the CO oxidation products region. The spectra recorded after admission of gases to Pt/TiO_2 was added for comparison. This spectrum **Figure 11(a)** shows different peaks characteristic of linear $\text{Pt}^0\text{-CO}$ (2077 cm^{-1}), CO absorption peak on $\beta\text{-Ti}^{4+}$ (2187 cm^{-1}), NCO species adsorbed on different sites (2217 and 2236 cm^{-1}) and finally physisorbed CO_2 (2350 cm^{-1}). Addition of Ce with 0.05 and 0.1% did not change the peak positions however it caused drastic changes in the intensity of all the peaks since the peaks intensity was maximum in $\text{PtCe}_{0.1}/\text{TiO}_2$ sample. Increasing Ce content to 0.5% leads to the decrease of the peak intensity and all the peaks (except CO absorption peak on $\beta\text{-Ti}^{4+}$) disappeared after raising the Ce content to 1% . As previously discussed, according to Di Monte *et al.* [33], the formation of isocyanate requires the presence of platinum group metals in the catalyst. The decrease of NCO and CO_2 with increasing Ce and the vanish of the adsorption peaks of $\text{Pt}^{\text{n+}}\text{-CO}$ indicate that Ce atoms may block Pt sites at Ce/TiO_2 ratio more than 0.1% and it totally mask Pt sites when Ce/TiO_2 ratio is 1% . Consequently, neither NCO nor CO_2 could be formed. As a result, the optimum ratio of Ce in Pt/TiO_2 to reduce NO and oxidize CO is being

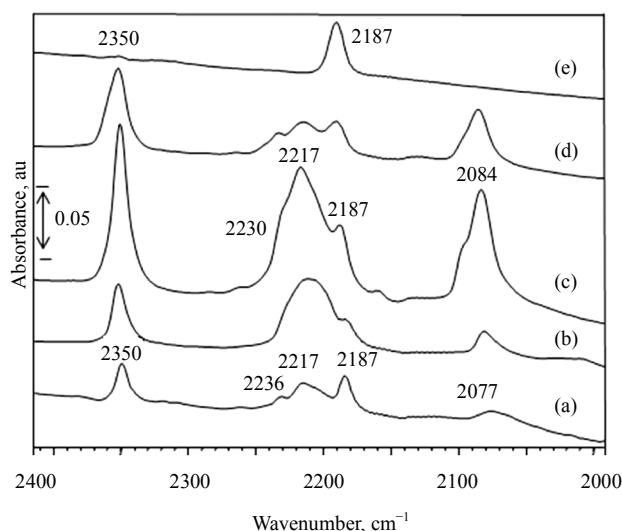


Figure 11. FTIR spectra after admission of gas mixture ($\text{NO} + \text{CO}$; 7:7) on $\text{PtCe}_x/\text{TiO}_2$ at different temperatures. (a) $x = 0$; (b) $x = 0.05$; (c) $x = 0.1$; (d) $x = 0.5$; and (e) $x = 1$.

0.1% .

It is noticed that, NCO was not detected after admission of $\text{NO} + \text{CO}$ over ($\text{PtCe}_1/\text{TiO}_2$, $\text{Ce}_{0.1}/\text{TiO}_2$ and TiO_2) and also after admission of ($\text{NO} + \text{CO} + \text{H}_2\text{O}$) over $\text{PtCe}_{0.1}/\text{TiO}_2$. In the former case, we could not observe any peak due to $\text{Pt}^{\text{n+}}\text{-CO}$ and in the later case we could not observe any peak due to $\text{Ti}^{4+}\text{-CO}$. However, we observed NCO after admission of ($\text{NO} + \text{CO}$) over Pt/TiO_2 and $\text{PtCe}_{0.1}/\text{TiO}_2$. In these cases, we observed both of $\text{Pt}^{\text{n+}}\text{-CO}$ and $\text{Ti}^{4+}\text{-CO}$ as well. From forgoing results, it is concluded that the presence of the mutual sites $\text{Pt}^{\text{n+}}$ and Ti^{4+} is crucial for the formation of NCO as a result of NO reduction. Additionally, the activity of $\text{PtCe}_{0.1}/\text{TiO}_2$ was higher than Pt/TiO_2 , indicating that Ce enhances the reaction towards NO reduction and forms NCO .

4. Conclusion

Platinum and cerium supported TiO_2 catalysts were successfully prepared by incipient wetness impregnation method in the particle size range of $19 - 22\text{ nm}$. Different reductive/oxidative species were observed after adsorption of NO and/or CO gasses. The presented results instantly allowed us to estimate the chemisorbed species after the admission of $\text{NO} + \text{CO}$ gas mixture and their interactions on Pt and Ce -containing catalysts supported on TiO_2 . The formation of both NCO and CO_2 was parallel indicating that their formation belongs to the same mechanism which is not certain until now. It was found that, the presence of both Pt sites and Ti^{4+} is important for NO reduction and NCO formation. Addition of Ce increased the formation of both NCO and CO_2 and it was optimum Ce/TiO_2 ratio of 0.1% .

REFERENCES

- [1] J. Beheshtian, M. Kamfiroozi, Z. Bagheri and A. Ahmadi, "Computational Study of CO and NO Adsorption on Magnesium Oxide Nanotubes," *Physica E*, Vol. 44, No. 3, 2011, pp. 546-549.
<http://dx.doi.org/10.1016/j.physe.2011.09.016>
- [2] B. Z. Sun, W. K. Chen, J. D. Zheng and C. H. Lu, "Roles of Oxygen Vacancy in the Adsorption Properties of CO and NO on Cu₂O(1 1 1) Surface: Results of a First-Principles Study," *Applied Surface Science*, Vol. 255, No. 5, 2008, pp. 3141-3148.
<http://dx.doi.org/10.1016/j.apsusc.2008.09.005>
- [3] R. L. Keiski, M. Härkönen, A. Lahti, T. Maunula, A. Savimäki and T. Slotte, "An Infrared Study of CO and NO Adsorption on Pt, Rh, Pd 3-Way Catalysts, Catalysis and Automotive Pollution Control III," *Studies in Surface Science and Catalysis*, Vol. 96, 1995, pp. 85-95.
[http://dx.doi.org/10.1016/S0167-2991\(06\)81421-7](http://dx.doi.org/10.1016/S0167-2991(06)81421-7)
- [4] E. Ivanova, M. Mihaylov, F. Thibault-Starzyk, M. Daturi and K. Hadjiivanov, "FTIR Spectroscopy Study of CO and NO Adsorption and Co-Adsorption on Pt/TiO₂," *Journal of Molecular Catalysis A*, Vol. 274, No. 1-2, 2007, pp. 179-184.
<http://dx.doi.org/10.1016/j.molcata.2007.05.006>
- [5] E. Guglielminotti and F. Boccuzzi, "Spectroscopic Characterization of the CeO₂/TiO₂ and Rh-CeO₂/TiO₂ Systems: CO Adsorption and NO-CO, NO-C₃H₈ Reactions," *Journal of Molecular Catalysis A*, Vol. 104, No. 3, 1996, pp. 273-283.
[http://dx.doi.org/10.1016/1381-1169\(95\)00180-8](http://dx.doi.org/10.1016/1381-1169(95)00180-8)
- [6] I. D. González, R. M. Navarro, W. Wen, N. Marinkovic, J. A. Rodruigé, F. Rosa and J. L. G. Fierro, "A Comparative Study of the Water Gas Shift Reaction over Platinum Catalysts Supported on CeO₂, TiO₂ and Ce-Modified TiO₂," *Catalysis Today*, Vol. 149, No. 3-4, 2010, pp. 372-379.
<http://dx.doi.org/10.1016/j.cattod.2009.07.100>
- [7] I. Malpartida, E. Ivanova, M. Mihaylov, K. Hadjiivanov, V. Blasin-Aube, O. Marie and M. Daturi, "CO and NO Adsorption for the IR Characterization of Fe²⁺ Cations in Ferrierite: An Efficient Catalyst for NO_x SCR with NH₃ as Studied by Operando IR Spectroscopy," *Catalysis Today*, Vol. 149, No. 3-4, 2010, pp. 295-303.
<http://dx.doi.org/10.1016/j.cattod.2009.09.015>
- [8] P. Klug and L. E. Alexander, "Direction Procedures for Polycrystalline and Amorphous Materials," Wiley, New York, 1954.
- [9] Q. H. Zhang, L. Gao and J. K. Guo, "Effects of Calcination on the Photocatalytic Properties of Nanosized TiO₂ Powders Prepared by TiCl₄ Hydrolysis," *Applied Catalysis B*, Vol. 26, No. 3, 2000, pp. 207-215.
[http://dx.doi.org/10.1016/S0926-3373\(00\)00122-3](http://dx.doi.org/10.1016/S0926-3373(00)00122-3)
- [10] L. Q. Jing, X. J. Sun, B. F. Xin, B. Q. Wang, W. M. Cai and H. G. Fu, "The Preparation and Characterization of La Doped TiO₂ Nanoparticles and Their Photocatalytic Activity," *Journal of Solid State Chemistry*, Vol. 177, No. 10, 2004, pp. 3375-3382.
<http://dx.doi.org/10.1016/j.jssc.2004.05.064>
- [11] A. Törnroona, M. Skoglundh, P. Thormählen, E. Fridell and E. Jobson, "Low Temperature Catalytic Activity of Cobalt Oxide and Ceria Promoted Pt and Pd: Influence of Pretreatment and Gas Composition," *Applied Catalysis B*, Vol. 14, No. 1-2, 1997, pp. 131-145.
[http://dx.doi.org/10.1016/S0926-3373\(97\)00018-0](http://dx.doi.org/10.1016/S0926-3373(97)00018-0)
- [12] Z. Jiang, W. Huang, H. Zhao, Z. Zhang, D. Tan and X. Bao, "Dispersion and Site-Blocking Effect of Molybdenum Oxide for CO Chemisorption on the Pt(1 1 0) Substrate," *Journal of Molecular Catalysis A*, Vol. 268, No. 1-2, 2007, pp. 213-220.
<http://dx.doi.org/10.1016/j.molcata.2006.12.024>
- [13] C. Te Hsieh, W. S. Fan, W. Y. Chen and J. Y. Lin, "Adsorption and Visible-Light-Derived Photocatalytic Kinetics of Organic Dye on Co-Doped Titania Nanotubes Prepared by Hydrothermal Synthesis," *Separation and Purification Technology*, Vol. 67, No. 3, 2009, pp. 312-318.
<http://dx.doi.org/10.1016/j.seppur.2009.03.041>
- [14] W. Y. Teoh, R. Amal, L. Madler and S. E. Pratsinis, "Flame Sprayed Visible Light Active Fe-TiO₂ for Photomineralisation of Oxalic Acid," *Catalysis Today*, Vol. 120, No. 2, 2007, pp. 203-213.
<http://dx.doi.org/10.1016/j.cattod.2006.07.049>
- [15] M. Mihaylov, K. Chakarova and K. Hadjiivanov, "Formation of Carbonyl and Nitrosyl Complexes on Titania and Zirconia-Supported Nickel: FTIR Spectroscopy Study," *Journal of Catalysis*, Vol. 228, No. 2, 2004, pp. 273-281.
<http://dx.doi.org/10.1016/j.jcat.2004.08.039>
- [16] I. Tankov, W. H. Cassinelli, J. M. C. Bueno, K. Arishtirova and S. Damyanova, "DRIFTS Study of CO Adsorption on Praseodymium Modified Pt/Al₂O₃," *Applied Surface Science*, Vol. 259, 2012, pp. 831-839.
<http://dx.doi.org/10.1016/j.apsusc.2012.07.138>
- [17] K. Pokrovski, K. T. Jung and A. T. Bell, "Investigation of CO and CO₂ Adsorption on Tetragonal and Monoclinic Zirconia," *Langmuir*, Vol. 17, No. 14, 2001, pp. 4297-4303.
<http://dx.doi.org/10.1021/la001723z>
- [18] Z. M. El-Bahy, A. I. Hanafy, M. M. Ibrahim and M. Anpo, "In Situ FTIR Studies of CO Oxidation over Fe-Free and Fe-Promoted PtY Catalysts: Effect of Water Vapor Addition," *Journal of Molecular Catalysis A*, Vol. 344, No. 1-2, 2011, pp. 111-121.
<http://dx.doi.org/10.1016/j.molcata.2011.05.008>
- [19] S. D. Ebbesen, B. L. Mojet and L. Lefferts, "In Situ ATR-IR Study of CO Adsorption and Oxidation over Pt/Al₂O₃ in Gas and Aqueous Phase: Promotion Effects by Water and pH," *Journal of Catalysis*, Vol. 246, No. 1, 2007, pp. 66-73.
<http://dx.doi.org/10.1016/j.jcat.2006.11.019>
- [20] K. Kinoshita, "Carbon, Electrochemical and Physical Properties," Wiley, New York, 1988.
- [21] F. Bozon-Verduraz and A. Bensalem, "IR Studies of Cerium Dioxide: Influence of Impurities and Defects," *Journal of the Chemical Society, Faraday Transactions*, Vol. 90, No. 4, 1994, pp. 653-657.
<http://dx.doi.org/10.1039/ft9949000653>
- [22] C. Shengzhou, H. Zou, Z. Liu and W. Lin, "DRIFTS Study of Different Gas Adsorption for CO Selective Oxidation on Cu-Zr-Ce-O Catalysts," *Applied Surface Science*, Vol. 255, No. 15, 2009, pp. 6963-6967.
<http://dx.doi.org/10.1016/j.apsusc.2009.03.021>

- [23] D. B. Akolekar and S. K. Bhargava, "Adsorption of NO and CO on Silver-Exchanged Microporous Materials," *Journal of Molecular Catalysis A*, Vol. 157, No. 1-2, 2000, pp. 199-206. [http://dx.doi.org/10.1016/S1381-1169\(00\)00055-8](http://dx.doi.org/10.1016/S1381-1169(00)00055-8)
- [24] Q. Yu, L. Liu, L. Dong, D. Li, B. Liu, F. Gao, K. Sun, L. Dong and Y. Chen, "Effects of Ce/Zr Ratio on the Reducibility, Adsorption and Catalytic Activity of CuO/Ce_xZr_{1-x}O₂/γ-Al₂O₃ Catalysts for NO Reduction by CO," *Applied Catalysis B*, Vol. 96, No. 3-4, 2010, pp. 350-360. <http://dx.doi.org/10.1016/j.apcatb.2010.02.032>
- [25] T. Nakatsuji, T. Yamaguchi, N. Sato and H. Ohno, "A Selective NO_x Reduction on Rh-Based Catalysts in Lean Conditions Using CO as a Main Reductant," *Applied Catalysis B*, Vol. 85, No. 1-2, 2008, pp. 61-70. <http://dx.doi.org/10.1016/j.apcatb.2008.06.024>
- [26] B. Azambre, L. Zenboudy, F. Delacroix and J. V. Weber, "Adsorption of NO and NO₂ on Ceria-Zirconia of Composition Ce_{0.69}Zr_{0.31}O₂: A DRIFTS Study," *Catalysis Today*, Vol. 137, No. 2-4, 2008, pp. 278-282. <http://dx.doi.org/10.1016/j.apcatb.2008.06.024>
- [27] C. Morterra and G. Magnacca, "A Case Study: Surface Chemistry and Surface Structure of Catalytic Aluminas, as Studied by Vibrational Spectroscopy of Adsorbed Species," *Catalysis Today*, Vol. 27, No. 3-4, 1996, pp. 497-532. [http://dx.doi.org/10.1016/0920-5861\(95\)00163-8](http://dx.doi.org/10.1016/0920-5861(95)00163-8)
- [28] K. I. Hadjiivanov and G. N. Vayssilov, "Characterization of Oxide Surfaces and Zeolites by Carbon Monoxide as an IR Probe Molecule," *Advances in Catalysis*, Vol. 47, 2002, pp. 307-511. [http://dx.doi.org/10.1016/0920-5861\(95\)00163-8](http://dx.doi.org/10.1016/0920-5861(95)00163-8)
- [29] O. S. Alexeev, S. Krishnamoorthy, C. Jensen, M. S. Ziebarth, G. Yaluri, T. G. Roberie and M. D. Amiridis, "In Situ FTIR Characterization of the Adsorption of CO and Its Reaction with NO on Pd-Based FCC Low NO_x Combustion Promoters," *Catalysis Today*, Vol. 127, No. 1-4, 2007, pp. 189-198. <http://dx.doi.org/10.1016/j.cattod.2007.05.003>
- [30] F. Solymosi and T. Bansagi, "Infrared Spectroscopic Study of the Isocyanate Surface Complex over Cu-ZSM-5 Catalysts," *Journal of Catalysis*, Vol. 156, No. 1, 1995, pp. 75-84. <http://dx.doi.org/10.1006/jcat.1995.1233>
- [31] R. Dumpelmann, N. W. Cant and D. L. Trimm, "Formation of Isocyanic Acid during the Reaction of Mixtures of NO, CO and H₂ over Supported Platinum Catalysts," *Applied Catalysis B*, Vol. 6, No. 4, 1995, pp. L291-L296. [http://dx.doi.org/10.1016/0926-3373\(95\)00024-0](http://dx.doi.org/10.1016/0926-3373(95)00024-0)
- [32] A. M. Sica and C. E. Giola, "Interaction of CO, NO and NO/CO over Pd/γ-Al₂O₃ and Pd-WO_x/γ-Al₂O₃ Catalysts," *Applied Catalysis A*, Vol. 239, No. 1-2, 2003, pp. 121-139. [http://dx.doi.org/10.1016/S0926-860X\(02\)00380-0](http://dx.doi.org/10.1016/S0926-860X(02)00380-0)
- [33] R. Di Monte, J. Kaspar, P. Fornasiero, M. Graziani, C. Pazéand and G. Gubitosa, "NO Reduction by CO over Pd/Ce_{0.6}Zr_{0.4}O₂/Al₂O₃ Catalysts: In Situ FT-IR Studies of NO and CO Adsorption," *Inorganica Chimica Acta*, Vol. 334, 2002, pp. 318-326. [http://dx.doi.org/10.1016/S0020-1693\(02\)00800-9](http://dx.doi.org/10.1016/S0020-1693(02)00800-9)
- [34] H. Arai and H. Tominaga, "An Infrared Study of Nitric Oxide Adsorbed on Rhodium-Alumina Catalyst," *Journal of Catalysis*, Vol. 43, No. 1-3, 1976, pp. 131-142. [http://dx.doi.org/10.1016/0021-9517\(76\)90300-6](http://dx.doi.org/10.1016/0021-9517(76)90300-6)
- [35] L. Liu, B. Liu, L. Dong, J. Zhu, H. Wan, K. Sun, B. Zhao, H. Zhu, L. Dong and Y. Chen, "In Situ FT-Infrared Investigation of CO or/and NO Interaction with CuO/Ce_{0.67}Zr_{0.33}O₂ Catalysts," *Applied Catalysis B*, Vol. 90, No. 3-4, 2009, pp. 578-586. <http://dx.doi.org/10.1016/j.apcatb.2009.04.019>
- [36] K. Chakarova, M. Mihaylov and K. Hadjiivanov, "FTIR Spectroscopic Study of CO Adsorption on Pt-H-ZSM-5," *Microporous and Mesoporous Materials*, Vol. 81, No. 1-3, 2005, pp. 305-312. <http://dx.doi.org/10.1016/j.micromeso.2005.01.033>
- [37] K. Chakarova, M. Mihaylov and K. Hadjiivanov, "Polycarbonyl Species in Pt/H-ZSM-5: FTIR Spectroscopic Study of ¹²CO-¹³CO Co-Adsorption," *Catalysis Communications*, Vol. 6, No. 7, 2005, pp. 466-471. <http://dx.doi.org/10.1016/j.catcom.2005.04.007>
- [38] K. Chakarova, K. Hadjiivanov, G. Atanasova and K. Tenchev, "Effect of Preparation Technique on the Properties of Platinum in NaY Zeolite: A Study by FTIR Spectroscopy of Adsorbed CO," *Journal of Molecular Catalysis A*, Vol. 264, No. 1-2, 2007, pp. 270-279. <http://dx.doi.org/10.1016/j.molcata.2006.09.040>
- [39] S. H. Oh and C. C. Eickel, "Influence of Metal Particle Size and Support on the Catalytic Properties of Supported Rhodium: CO+O₂ and CO+NO Reactions," *Journal of Catalysis*, Vol. 128, No. 2, 1991, pp. 526-536. [http://dx.doi.org/10.1016/0021-9517\(91\)90310-Z](http://dx.doi.org/10.1016/0021-9517(91)90310-Z)
- [40] S. H. Oh, "Effects of Cerium Addition on the CO+NO Reaction Kinetics over Alumina-Supported Rhodium Catalysts," *Journal of Catalysis*, Vol. 124, No. 2, 1990, pp. 477-487. [http://dx.doi.org/10.1016/0021-9517\(90\)90194-O](http://dx.doi.org/10.1016/0021-9517(90)90194-O)
- [41] M. Paulis, H. Peyrard and M. Montes, "Influence of Chlorine on the Activity and Stability of Pt/Al₂O₃ Catalysts in the Complete Oxidation of Toluene," *Journal of Catalysis*, Vol. 199, No. 1, 2001, pp. 30-40. <http://dx.doi.org/10.1006/jcat.2000.3146>
- [42] T. M. Salama, Z. M. El-Bahy and F. I. Zidan, "Aqueous H₂O₂ as an Oxidant for CO over Pt- and Au-NaY Catalysts," *Journal of Molecular Catalysis A*, Vol. 264, No. 1-2, 2007, pp. 128-134. <http://dx.doi.org/10.1016/j.molcata.2006.08.003>
- [43] A. Parinyaswan, S. Pongstabodee and A. Luengnarue-mitchai, "Catalytic Performances of Pt-Pd/CeO₂ Catalysts for Selective CO Oxidation," *International Journal of Hydrogen Energy*, Vol. 31, No. 13, 2006, pp. 1942-1949. <http://dx.doi.org/10.1016/j.ijhydene.2006.05.002>
- [44] S. D. Ebbesen, B. L. Mojet and L. Lefferts, "In situ ATR-IR Study of CO Adsorption and Oxidation over Pt/Al₂O₃ in Gas and Aqueous Phase: Promotion Effects by Water and pH," *Journal of Catalysis*, Vol. 246, No. 1, 2007, pp. 66-73. <http://dx.doi.org/10.1016/j.jcat.2006.11.019>